Austin Journal of Biosensors & Bioelectronics

Open Access

Austin Publishing Group

Research Article

Computer Modeling and Simulation of Stromal Tumor and Its Ablation Method in the Small Intestine

Shirzadfar H*, Shahbazi M and Ghasemi F
Department of Biomedical Engineering, Sheikhbahaee University, Iran

***Corresponding author:** Hamidreza Shirzadfar, Department of Biomedical Engineering, Sheikhbahaee University, Isfahan, Iran

Received: October 11, 2018; **Accepted:** November 12, 2018; **Published:** November 19, 2018

Abstract

Gastrointestinal Stromal Tumors (GISTs), commonly referred to as GISTs, are the most common gastrointestinal mesenchyme tumors. The prevalence of sexually transmitted GIST tumors in men and women is roughly the same. These tumors are commonly seen in people over the age of 50 years and are not common in ages less than 40 years and much rare in children. The most common site of GIST is in the stomach and then the small intestine. The most common clinical symptom of GIST tumors, seen in about 50% of patients, is prolonged gastrointestinal bleeding. Other symptoms include abdominal pain, anemia with uncertain origins, weight loss and acute vomiting. Sometimes these tumors are found in clinical examinations as abdominal masses. In general, treating GIST tumors is three: Surgery, Intelligent Therapies and a combination of Surgery and Intelligent Therapies. A therapeutic approach to eliminating cancerous tumors from healthy tissues is to heat the malignant tissue to a critical temperature in order to kill cancer cells. This method is used in this paper.

Keywords: Gastrointestinal Stromal Tumors (GISTs); Small intestine; RF probe; FEM analysis; Bio-heat equation; COMSOL multiphysics

Introduction

Gastrointestinal Stromal Tumors (GISTs) are the most common gastrointestinal mesenchyme tumors and are the result of gene mutations that usually occur in the mucosal layer and from the underlying or muscular tissues of the stomach, and grow slowly [1-5]. About 70% of cases are gastric tumors composed of spinal cord, and about 30% of them are epithelioid cells that are round and multifaceted. The remaining 10% is a mixture of spindly and epithelioid cells called pleomorphic cells [6]. The involvement of the digestive tract due to neoplastic alteration is a sample of the interstitial Cajal cell, which is commonly found in both muscle layers of the intestinal wall. GIST tumors located in the small intestine usually present with abdominal pain, signs of partial obstruction or gastrointestinal bleeding, and sometimes imitate biliary colic symptoms.

Carcinogenesis appears to originate in response to a mutation activating the membrane receptor KIT or PDGFRA. After this mutation, KIT, even in the absence of a ligand, becomes an active metabolism, leading to the growth of uncontrolled cells and the development of GIST. Too much KIT is special for a GIST. To detect immunohistochemistry (CD117) and to predict response to treatment, tyrosine kinase inhibitors are used [7].

In 85% of GIST cases, tumor behavior is guided by kit mutations. The C-kit receptor tyrosine kinase gene is coded for trans-membrane receptor. This is a growth factor receptor, which is called the causative factor. There is often a mutation in the C-kit gene; however, it can sometimes be a defect in the pathway to the C-kit enzyme's structural activity. The mutations occur in the exons (9-17) of this gene. 10% GIST has a mutation in the PDGFRA gene, which is also the receptor gene for tyrosine kinase. The mutations are seen in exons 12, 14 and 18 of the PDGFRA gene. Rarely, BRAF kinase mutations are seen. The inhibition of these Tyrosine Kinases (TKs) has altered the treatment of these tumors, since they are currently exposed to the specific purpose of treating TK inhibitors.

The remarkable sensitivity of these tumors to new tyrosine kinase receptor inhibitors such as imatinib, mesylate and sunitinib has significantly changed the management and prognosis of these tumors. Some GISTS do not have C-kit mutations or PDGFRA and carry these types of mutations in all acute parts of the C-kit and PDGFRA genes. Recent discoveries highlighted mutations in conventional genes such as NF1, SDH, CD34, nestin, SMA, caldesmon, calponin, vimentin, and precancerous muscle actin [8].

GIST lesions may be presented clinically as sub-mucosal lesions, internal lesions, or lesions of a subset of different sizes. In most cases, these tumors are benign and rarely seek malignancy, but if their withdrawal is incomplete, tumors may recur and further grow [7].

The incidence of GIST is generally about 10 to 20 per million populations. Of these, 20 to 30% are malignant. The prevalence of sexually transmitted GIST tumors in men and women is roughly the same. These tumors are commonly seen in people over the age of 50 years and are not common in ages less than 40 years and are rare in children, but it should be noted that the peak of these tumors is in the fifth and sixth decades of life. In some studies, the highest age range for diagnosis of these tumors was between the ages of 55 and 63 [9].

Most GIST occurs in the stomach and only 30% occurs within the small intestine [10]. Small intestinal gastrointestinal tract may be located along the length of the intestine and anywhere. About 10% of patients with GIST tumors have seen other malignancies, including renal cell carcinoma, stomach and lung. There are also a few reports of a family of GIST tumors with family backgrounds, which can be found in families with a type 1 neurofibromatosis disease that

Citation: Shirzadfar H, Shahbazi M and Ghasemi F. Computer Modeling and Simulation of Stromal Tumor and Its Ablation Method in the Small Intestine. Austin J Biosens & Bioelectron. 2018; 4(1): 1032.

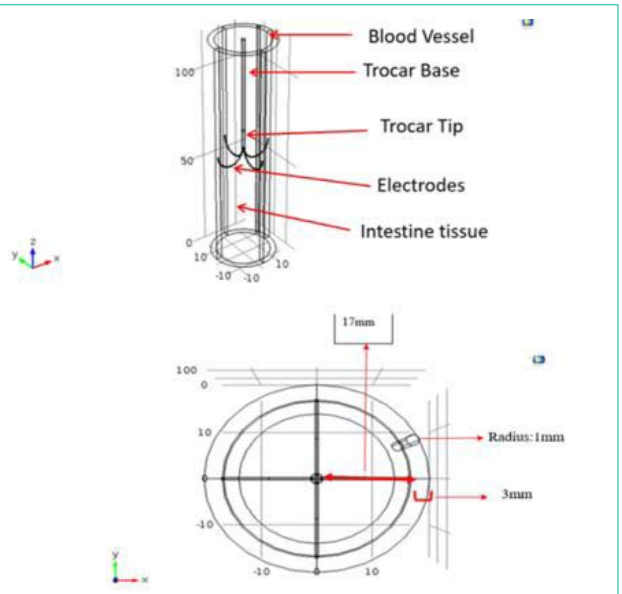

Figure 1: An overview of the model and dimensions considered for the model.

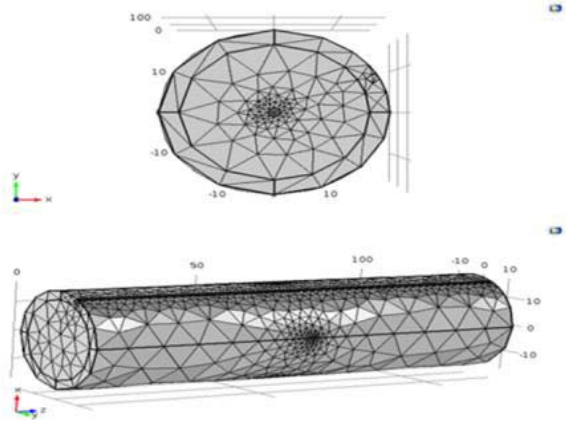

Figure 2: The 3D Geometry and physical dimension of model.

increases the risk of GIST tumors in these families [11].

Currently, the most commonly used risk is the classification, tumor size, site of origin and methionine index (the ratio of the number of mitosis cells (cell division) to the total number of cells). Subsequently, the integration of risk estimation with tumor detachment has been completed and the sizes of the tumor and mitosis indicator are considered as permanent variables. Gene mutation states have been suggested as a potential risk factor for GIST tumors, but today there are no risk categories. An Incidence risk categorization tool is used to suggest follow-up strategies in the guidelines [12].

In rare cases, GIST tumors are seen in many members of a family. Age factors are also considered as a risk factor for these tumors, as most of the diagnosed patients are over the age of 50 [9].

Clinical protests

More than 80% of these tumors are seen primarily in the gastrointestinal tract, and about 10% of these tumors are primarily seen in the peritoneum and pelvic space. About 40% to 70% of GIST tumors are found in the stomach and are commonly found in the stomach fundus, which make up only 1 to 3% of gastric neoplasms. About 20% to 50% of GIST tumors are found in the small intestine and typically in JeJnum. Only about 5% of these tumors are found in the large intestine and rectum, and less than 5% of these tumors are seen in the esophagus [13]. Of course, sporadically, GIST tumors have been seen in the reproductive system, pelvis, appendix, gallbladder, mesentery, or omentum [14-18]. The clinical manifestations of these tumors are not specific and depend on the location of the tumor. About 10% to 30% of these tumors are completely asymptomatic, so they are accidentally found during endoscopic, radiological examinations and surgical interventions. The most common clinical symptom of GIST tumors, seen in about 50% of patients, is prolonged gastrointestinal bleeding. Other symptoms include abdominal pain (about 20% to 50% of patients), and anemia with uncertain origin, weight loss and acute vomiting [19,20]. Sometimes these tumors are found in clinical examinations as abdominal masses. GIST tumors present in the esophagus are usually small and asymptomatic, but larger tumors can exhibit dysphagia, Odynophagia, posterior pain, Hmaatmz, and weight loss. Meanwhile, they can accidentally appear as an unusual mediastina shadow in the chest photo. Gastric tumors located in the stomach can cause epigastria pain, loss of appetite, nausea, and vomiting and weight loss. Gastric tumors located in the small intestine usually present with abdominal pain, signs of relative obstruction or gastrointestinal bleeding, and sometimes imitate biliary colic symptoms. Tumors located in the second part of the intestinal duodenum may cause jaundice. Large intestinal lesions show themselves with abdominal pain and changes in bowel habits. In addition, these tumors may cause blockage and less perforation [5, 6, 21-23]. Metastasis of GIST tumors is usually limited to the abdominal cavity. In 54% of cases, metastases to the liver can be isolated in the liver or with lesions developed in the peritoneum. The metastatic lesions of the GIST tumor in the liver are usually large and numerous and are found in both liver lobes. The second most common site of metastasis is peritoneum [24]. GIST tumors rarely metastasize into the lungs (usually rectum tumors), pleura and bone curtains.

Diagnosis

There are various diagnostic methods for GIST tumors. Small and asymptomatic tumorous lesions are usually found accidentally during endoscopy for a variety of reasons. Therefore, endoscopy is one of the diagnostic methods and also the study of GIST tumors. In endoscopic studies, GIST tumors are usually altered in the underlying mucosa, which are seen prominently in the lumen of the gastrointestinal tract. The mucus that covers the tumor may be healthy, but it can be slightly damaged or even wounded. In addition, a simple chest graph can help with endoscopy, especially in the large GIST tumors located at the esophagus. CT scan findings show these tumors as solid tumors that are strengthened by intravenous contrast media [25,26]. In addition to endoscopy and CT scan, endo-sonography also plays a prominent role in the diagnosis of these tumors. Generally, in the endo-sunography, GIST tumors are identified as Hypo acoustic masses by the origin of muscle layers (typically mucosal muscle or the main muscle layer). The suggestive patterns of the malignant potential of GIST tumors are greater than 4 cm, irregular margins, cysts and non-homogeneous echoes are well defined in endosonography [6].

It should be noted that the final and definitive diagnosis is based

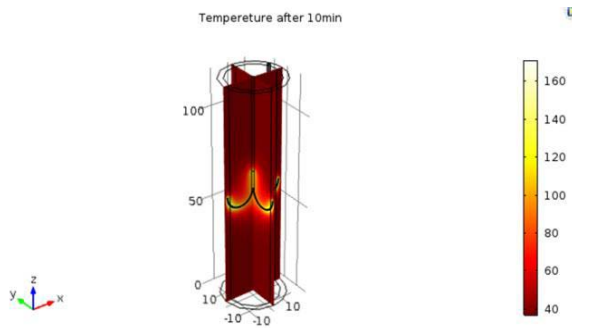

Figure 3: Temperature variations in the tissue around the electrode.

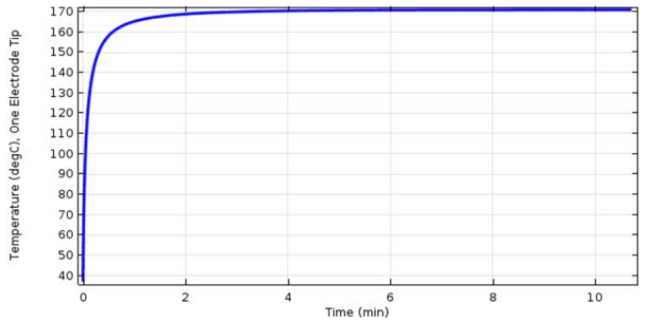

Figure 4: Temperature variations at the tip of one of the electrode arms.

on the histological examination of the biopsy sample taken from the tumor. The biopsy sample can be done under endoscopy as well as endosonography [6].

PET-FDG scan can also be used as a useful and helpful diagnostic tool along with other diagnostic methods of the GIST tumor [6].

Prognosis

To determine the prognosis of GIST tumors, diagnostic interventions including chest rhythm, ultrasound, CT scans, and abdominal endo-sunography should be performed to disprove or confirm the spread of the tumor, as well as identify the location of the tumor and its association with surrounding structures. About 20% of the GIST malignant tumors are detected when they are widely distributed. This is especially true for small GIST lesions that have been asymptomatic for a long time and have been accidentally detected. The average duration for clinical symptoms is approximately 4 to 6 months, and the average duration for spreading the tumor is 2 years. Asymptomatic tumors, in most cases, are associated with gastric and duodenum tumors. The highest survival time among GIST tumors is related to tumors of the stomach. Another point is that malignant GIST tumors are more common in the distal areas of the gastrointestinal tract [6,14]. The prognosis of GIST tumors is dependent on the size of the tumor and the number of mitosis in each microscopic field. Tumors of less than 2 cm in size and mitosis less than 5 in the microscopic field of 50 are typically benign and have a good prognosis. Tumors with a size less than 5 cm and mitosis of 6 to 10 or a size of 5 to 10 cm and mitosis of less than 5 have a moderate degree of malignancy. Tumors larger than 10 cm in size and with any number of mitoses and tumors with mitosis above 10 and of any size have a high degree of malignancy. In addition, malignant tumors of GIST in women are better than males [6,27]. Patients with Advanced GIST tumors will have about 9 to 20 months.

Treatment

In general, three methods are used to treat GIST tumors: Surgery, Therapy Targeted, and a combination of Surgery and Intelligent Therapy. Surgery is generally recognized as the most important basis for treatment in patients with GIST. In those whose tumors are not surgical or metastasis, they are treated with smart or sometimes combined therapy. Common chemotherapy used in soft tissue sarcomas is not effective in patients with GIST. Also, the use of radiotherapy in patients with GIST has limited effects [28,29].

Materials and Methods

One way to eliminate cancerous tumors from healthy tissues is to heat the malignant tissue to a critical temperature to kill cancer cells. In this method, four electrodes that carry electrical current into the tissue are used to generate local heat. The electric field electric heat source is known as heat resistance or heat Joule. The treatment process used to remove the tuber is 45 to 50°C [30]. Doing this requires a local source of heat that physicians create by placing a small electrical probe. In this research, the proposed method is simulated with the Comsol multiphysics finite element analysis software. Comsol software is used for this simulation as an analysis program because Comsol's multiphysics software is a complete simulation suite that allows users to simulate in 3D space. Comsol gives the user the opportunity to solve technical problems by choosing a physical environment. In the Comsol function section, all three steps are: preprocessing, processing, and post-processing processing. In this simulation, we used Bio-heat's transmission interface, an electrical current interface, and a multi-physical characteristic, an electromagnetic heating source, to implement a transient analysis. The standard temperature unit in COMSOL Multiphysics is Kelvin (K). The model uses a degree of centigrade that is better for bioequivalence models. Using FEM analyzes, we show the characteristics of the lesions created by a typical four-phase RF probe, which consists of four titanium-nickel electrodes and a stainless steel throat rod [30]. The lesion in the intestinal tissue without blood vessels is predictable. However, it indicates the inadequacy of the RF probe in heating tissue around large blood vessels. The presence of large blood vessels near the tumor has the following effects [30].

Since blood has a higher electrical conductivity, RF flow is absorbed from the RF probe. This causes the temperature to increase in the intestinal tissue between the electrode and the blood vessels due to the joule effect.

The blood flow in the large vein acts as a heat of the sun and eliminates heat from the surrounding tissue. The distance between the blood vessels from the tumor, the dominant factor, and the position determines the maximum tissue temperature.

The materials used to design the model and their characteristics are described in the (Table 1) for solving the environmental equations.

Simulation and Results

As shown in Figure 1, the probe is made of a Trocar (main bar) and four electrode straps. The wire is insulated electrically, except near the electrode arms. By applying electrical current through electrodes,

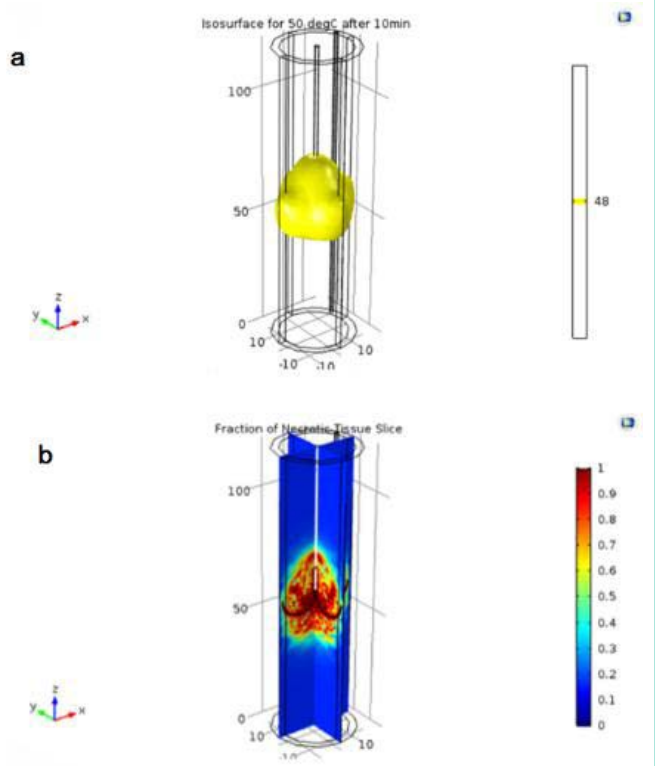

Figure 5: a) Showing the area of the cancerous tumor after 10 minutes at 48°C. Figure 5 (b) shows a fracture of tissue damage after completion of the process.

a strong electric field will be formed around the gland that results in the formation of a heat-resistant resistor in that area of the tissue.

In this model we almost divide the body tissue with a large cylinder with a thickness of 3mm and assume that its boundary temperature remains at 37°C throughout all stages and according to the explanations given above, a vessel with a radius of 1 mm is considered. The tumor is located near the center of the cylinder and has thermal properties similar to the surrounding tissue. Place the probe along the center line of the cylinder so that its electrodes are located in the area where the tumor is located [30]. In this model, we solve the above equations with given boundary conditions, so that the temperature field functions as a function of time to and we also show how the temperature increases with time in the tissue around the electrode. Figure 2 shows the 3D simulations.

The bio-heat equation controls heat transfer in the tissue

$$\delta_{ts}\rho\frac{\partial T}{\partial t}+\nabla.\left(-k\nabla T\right)=\rho_b C_b\omega_b\left(T_a-T\right)+Q_{met}+Q_{ext} \qquad (1)$$

Which δ_{ts} is a time scale factor; ρ is the density of tissue (kg/m^3). C is the special heat of tissue (J/(kg.K) and its thermal conductivity is (W/(m.K)). On the right side, ρ_b gives the density of blood (kg/m^3); C_b is the specific blood temperature (J/(kg.K), ω_b is its perfusion rate (1/s); T_b is the arterial temperature (K), while Q_{met} and Q_{ext} are the heat sources of space metabolism and heat (W/m^3) In this model, the environmental equation is also modeled for heat transfer in different sections of the probe with values appropriate for the specific heat C ((J/kg.K), and the thermal radiation K (W/(m.K). For this section all terms on the right are zero.

In addition to the heat transfer equation [31], this model examines the amount of damage that occurs in the tissue. This applies to the extent of tissue damage α during the process, based on the Arnenius equation:

$$\frac{d\alpha}{dt}=A\exp\left(-\frac{dE}{RT}\right) \qquad (2)$$

where A is the frequency factor (1/s) and dE is the active energy for the irreversible degradation reaction (J/mol). These two parameters are dependent on the type of tissue. θ_d The amount of deficit of the nicotine tissue that is expressed as:

$$\theta_d=1-\exp\left(-\alpha\right) \qquad (3)$$

In this regard, the parameter α indicates the degree of tissue degradation.

The electric current in this simulation is based on the electric current relationship as follows:

$$-\nabla.\left(\sigma\nabla V-J^e\right)Q_j \qquad (4)$$

where V is the potential, σ is the electrical conductivity, J^e is the produced external current density (A/m^2), Q_j is the current source (A/m^3). In this model, J^e and Q_j are zero. So it's simplified:

$$-\nabla.\left(\sigma\nabla V\right)=0 \qquad (5)$$

In the boundary conditions at the outer boundaries of the cylinder, the potential is considered to be 0, while the potential in the electrodes is equal to 22V. Boundary conditions for electric current are:

V = 0 on the walls of the cylinder

V = V0 on the electrode surfaces

n. (J1-J2) on all other borders

The boundary conditions for the environmental equation are:

T = Tb on the cylinder wall and blood vessel wall

$n.\left(k_1\nabla T_1-k_2\nabla T_2\right)=0$ On all internal borders

This model solves the above equations with given boundary conditions to obtain the temperature field as a function of time, and also shows how the temperature increases with time in the

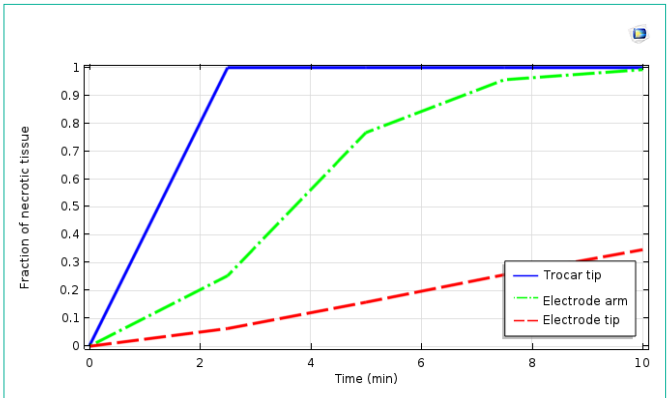

Figure 6: Changes made in three different locations from the degraded part of the tissue over time.

Table 1: The specification and properties of materials used in this investigation.

MATERIALS	PROPERTIES			
	Electrial conductivity(s/m)	Heat capacity at constant pressure(J/kg.K)	Thermal conductivity(W/m.K)	Density (kg/m^3)
Intestine Tissue	0.333	3750	0.5	1000
Blood vessel	0.667	4180	0.543	1000
Electrode	1.00E+08	840	18	6450
Trocar	4.00E+06	132	71	21500
Trocar base	1.00E-05	1045	0.026	70

surrounding tissue of the electrode. In (Figure 3), the temperature field is shown at the end of the 10-minute experiment. In (Figure 3), the temperature distribution at the end of the 10-minute experiment is shown. The symmetric temperature distribution is observed between the two sides of the probe. Places with the highest temperatures or "hot spots" were located adjacent to the electrodes.

Figure 4 shows the temperature at the tip of one of the electrode arms. Its temperature rises rapidly to reach around 150°C, Which reaches this steady state in less than 0.5 minutes and it is interesting to imagine the area where the cancer cells die, where the temperature reaches at least 48 degrees Celsius. We can visualize this area with a ground level for this temperature; Figure 5a shows one dimension after 10 minutes. Figure 5b shows a portion of the tissue degradation at the end of the test.

The Figure 6 shows the effect of tissue degradation at three different points above the electrode arm. It is observed that a faster necrosis occurs next to the electrode and the tip of the thruca. The blue line shows a higher rate of destruction of tumor cells in the intestine. The green line shows that more than 10% of the tumor cells in the liver are destroyed. The red line indicates that a small amount of tumor cells disappears after 10 minutes. Destruction was carried out at 48°C.

Conclusion

In this article, we studied the gastrointestinal mesenchyme tumor and examined such cases as clinical manifestations, prognosis and treatment of this type of tumor. Given the fact that the stromal tumor is in 50% of cases asymptomatic, infrared thermography can be used to detect it in the future (considering the application of thermography in the diagnosis of tumor types).

In this study after examining the characteristics of the stromal tumor, using FEM analysis, we showed the characteristics of lesions in the small intestinal tissue by a typical four-phase RF probe. Considering the ionized bowel model, we conclude that the small intestinal dimensions of the small intestine are related to the small intestinal anatomy, and in simulating it, we assume that the diameter of the lumen and the inner and outer radius are constant and the small intestinal parasites are neglected. According to the Bio-heat equation, heat transfer for tissue and considering the boundary conditions for the equation as well as the amount of damage to the tissue, to eliminate cancerous tumors from healthy tissues, to heat the malignant tissue to a critical temperature using an electrical current probe is needed and it is observed that within 10 minutes at 48-50°C, cancer cells are destroyed, while the rate of destruction in the electrode arm and the trocar rod is faster.

References

1. Ando N, Goto H, Niwa Y, Hirooka Y, Ohmiya N, Nagasaka T, et al. The diagnosis of GI stromal tumors with EUS-guided fine needle aspiration with immunohistochemical analysis. 2002; 55: 37-43.
2. Crosby JA, Catton CN, Davis A, Couture J, O'Sullivan B, Kandel R, et al. Malignant gastrointestinal stromal tumors of the small intestine: a review of 50 cases from a prospective database. 2001; 8: 50-59.
3. Cheuk W, Lee KC, Chan JK. C-kit immunocytochemical staining in the cytologic diagnosis of metastatic gastrointestinal stromal tumor. 2000; 44: 679-685.
4. Duffaud F, Blay JY. Gastrointestinal stromal tumors: biology and treatment. 2003; 65: 187-197.
5. Miettinen M, Sobin LH, Lasota J. Gastrointestinal stromal tumors of the stomach: a clinicopathologic, immunohistochemical, and molecular genetic study of 1765 cases with long-term follow-up. 2005; 29: 52-68.
6. Zawisza A, J Milewski, GJWWzgpMPE Rydzewska, Rydzewska G. Stromal tumors of the gastrointestinal tract. Termedia Medical Publishing. 2007: 103-113.
7. Pellino G, Marcellinaro R, Candilio G, De Fatico GS, Guadagno E, Campione S, et al. The experience of a referral centre and literature overview of GIST and carcinoid tumours in inflammatory bowel diseases. Int J Surg. 2016; 28: S133-S141.
8. Abbas F, Waseem Raja Dar, Muzamil Latief, Summyia Farooq, Manzoor Ahmad Parry, Peerzada Ziaulhaq, et al. Gastrointestinal Stromal Tumors: A Review. 2016.
9. Tran TJA. Davila JA, El-Serag HB. The epidemiology of malignant gastrointestinal stromal tumors: an analysis of 1,458 cases from 1992 to 2000. 2005; 100: 162.
10. Humenansky KM, Gulati R. Small bowel gastrointestinal stromal tumor disguised as an adnexal mass: a source for midgut volvulus. J Surg Case Rep. 2018; 2018: 157.
11. Yantiss RK, Rosenberg AE, Sarran L, Besmer P, Antonescu CR. Multiple gastrointestinal stromal tumors in type I neurofibromatosis: a pathologic and molecular study. 2005; 18: 475.
12. D'Ambrosio L, Palesandro E, Boccone P, Tolomeo F, Miano S, Galizia D, et al. Impact of a risk-based follow-up in patients affected by gastrointestinal stromal tumour. 2017; 78: 122-132.
13. Popiela T, Kulig J, JJGihkW Stachura, PZWL, Gastrointestinal neoplasms. 2006; 435.
14. Ruka W, et al. Contemporary management in patients with gastrointestinal stromal sarcomas (GIST-gastrointestinal stromal tumors). 2003; 53: 537-542.
15. Belics Z, Csapó Z, Szabó I, Pápay J, Szabó J, Papp Z. Large gastrointestinal stromal tumor presenting as an ovarian tumor. A case report. 2003. 48: 655-658.
16. Zighelboim I, Henao G, Kunda A, Gutierrez C, Edwards C. Gastrointestinal stromal tumor presenting as a pelvic mass. 2003; 91: 630-635.
17. Carlomagno G, Pasquale Beneduce. A gastrointestinal stromal tumor (GIST) masquerading as an ovarian mass. 2004; 2: 15.

18. Cai N, Morgenstern N, Patricia Wasserman. A case of omental gastrointestinal stromal tumor and association with history of melanoma. 2003; 28: 342-344.

19. Kim HC, Lee JM, Kim SH, Kim KW, Lee M, Kim YJ, et al. Primary gastrointestinal stromal tumors in the omentum and mesentery: CT findings and pathologic correlations. 2004; 182: 1463-1467.

20. Perego M, Strada E, Alvisi C, Ascari E. Gastrointestinal stromal tumor as the cause of intestinal hemorrhage: description of a clinical case. 1998; 13: 125-127.

21. Czupryniak L, Stanisław Sporny, Jacek W Kuroszczyk , J-ózef Drzewoski. Cystic gastrointestinal stromal tumor. 1999; 5: CS770-CS773.

22. Lucchetta MC, Liberati G, Petraccia L, Campanella J, Grassi M. Gastrointestinal stromal tumors: a seldom diagnosed cause of severe anemia. Dig Dis Sci. 2005; 50: 815-819.

23. D'amato G, Steinert DM, McAuliffe JC, Trent JC. Update on the biology and therapy of gastrointestinal stromal tumors. Cancer Control. 2005; 12: 44-56.

24. Miettinen M, Maarit Sarlomo-Rikala, Leslie H Sobin, Jerzy Lasota. Esophageal stromal tumors: a clinic pathologic, immunohistochemical, and molecular genetic study of 17 cases and comparison with esophageal leiomyomas and leiomyosarcomas. The American Journal of Surgical Pathology. 2000; 24: 211-222.

25. Hughes TP, Kaeda J, Branford S, Rudzki Z, Hochhaus A, Hensley ML, et al. Frequency of major molecular responses to imatinib or interferon alfa plus cytarabine in newly diagnosed chronic myeloid leukemia. 2003; 349: 1423-1432.

26. Ghanem N, Altehoefer C, Furtwängler A, Winterer J, Schäfer O, Springer O, et al. Computed tomography in gastrointestinal stromal tumors. 2003; 13: 1669-1678.

27. Fletcher CD, Berman JJ, Corless C, Gorstein F, Lasota J, Longley BJ, et al. Diagnosis of gastrointestinal stromal tumors: a consensus approach. 2002; 10: 81-89.

28. Ng E, R E Pollock, M F Munsell, E N Atkinson, M M Romsdahl. Prognostic factors influencing survival in gastrointestinal leiomyosarcomas. Implications for surgical management and staging. 1992; 215: 68.

29. Druker BJ, Nicholas B, Lydon. Lessons learned from the development of an abl tyrosine kinase inhibitor for chronic myelogenous leukemia. 2000; 105: 3-7.

30. Tungjitkusolmun S, ST Staelin, D Haemmerich, Jang-Zern Tsai, Hong Cao, JG Webster, et al. Three-dimensional finite-element analyses for radio-frequency hepatic tumor ablation. 2002; 49: 3-9.

31. Shirzadfar H, Shahbazi M, Ghasemi F. A Review of Recent Application of Medical Thermography in Human Body for Medical Diagnosis, SCIOL Biomedicine.

Austin J Biosens & Bioelectron - Volume 4 Issue 1 - 2018
ISSN : 2473-0629 | www.austinpublishinggroup.com

Citation: Shirzadfar H, Shahbazi M and Ghasemi F. Computer Modeling and Simulation of Stromal Tumor and Its Ablation Method in the Small Intestine. Austin J Biosens & Bioelectron. 2018; 4(1): 1032.